Author Manuscript

N^G,N^G-dimethylarginine dimethylaminohydrolase 1 expression is dispensable for cold- or diet-induced thermogenesis

Min-Jung Park[1,6], Junhyeong Lee[1,2,6], Bernadette B. Bagon[1], Merc Emil Matienzo[1,2], Sangyi Lim[1,2], Keon Kim[2,3], Chang-Min Lee[2,3], Jun Wu[4,5], Dong-il Kim[1,2*]

[1]Department of Veterinary Physiology, College of Veterinary Medicine, Chonnam National University, Gwangju 61186, Korea; [2]College of Veterinary Medicine and BK21 FOUR Program, Chonnam National University, Gwangju 61186, Korea; [3]Department of Veterinary Internal Medicine, College of Veterinary Medicine, Chonnam National University, Gwangju 61186, Korea; [4]Life Sciences Institute, University of Michigan, Ann Arbor, MI 48109, USA; [5]Department of Molecular and Integrative Physiology, University of Michigan Medical School, Ann Arbor, MI 48109, USA.

Correspondence: [*]Dong-il Kim, Department of Veterinary Physiology, College of Veterinary Medicine, Chonnam National University, Gwangju 61186, Korea.

Phone: +82-62-530-2832, Fax: +82-62-530-2809

E-mail: kimdi@chonnam.ac.kr

[6] These authors contributed equally to this work.

Abstract

This is the author manuscript accepted for publication and has undergone full peer review but has not been through the copyediting, typesetting, pagination and proofreading process, which may lead to differences between this version and the Version of Record. Please cite this article as doi: 10.1002/adbi.202300192.

This article is protected by copyright. All rights reserved.

Author Manuscript

Strategy to activate thermogenic adipocytes has therapeutic potential to overcome obesity as they dissipate surplus energy as heat through various mechanisms. N^G,N^G-dimethylarginine dimethylaminohydrolases (DDAHs) are enzymes involved in the nitric oxide (NO)-protein kinase G (PKG) signaling axis which increases thermogenic gene expression. However, the role of DDAHs in thermogenic adipocytes has not been elucidated. We generated adipocyte-specific *Ddah1* knockout mice by crossing *Ddah1*$^{fl/fl}$ mice with adiponectin Cre (AQ-Cre) recombinase mice. Adipocyte-specific DDAH1 overexpressing mice were generated using adeno-associated virus-double-floxed inverse open reading frame (AAV-DIO) system. These mice were analyzed under basal, cold exposure, or high-fat diet (HFD) conditions. Primary inguinal white adipose tissue (iWAT) cells from adipocyte-specific *Ddah1* knockout mice expressed comparable amounts of *Ucp1* mRNA. Adipocyte-specific DDAH1 overexpressing mice did not exhibit enhanced activation of thermogenic adipocytes. In addition, when these mice were exposed to cold environment or fed an HFD, their body temperature/weight and thermogenesis-related gene and protein expressions were unchanged. These findings indicate that DDAH1 does not play a role in either cold- or diet-induced thermogenesis. Therefore, adipocyte targeting DDAH1 gene therapy for the treatment of obesity is unlikely to be effective.

Keywords: DDAH1; obesity; thermogenesis; AAV-DIO; gene therapy

1. Introduction

Activation of thermogenic adipocytes is considered as a potential strategy to combat obesity [1]. There are at least two types of thermogenic adipocytes in mice, one of which is brown adipocytes located in specific depots like the interscapular region. The other type is beige adipocytes which sporadically arise within subcutaneous white adipose tissue by stimuli such as exposure to cold environments and activation of adrenergic receptor β3 (ADRB3) [2]. These adipocytes dissipate surplus energy as heat through various mechanisms [1]. One of the well characterized and efficient ways to stimulate these

This article is protected by copyright. All rights reserved.

Author Manuscript

cells is activation of ADRB3, which increases the cytosolic level of cyclic adenosine monophosphate (cAMP). cAMP binds and activates protein kinase A (PKA), which turns on the transcription of uncoupling protein 1 (UCP1) [2a]. As UCP1 breaks down the proton gradient generated by the electron transport chain, activation of the ADRB3-cAMP-PKA-UCP1 axis is anticipated to contribute to weight loss. Importantly, humans also possess thermogenic adipocytes responsive to ADRB3 agonists [3].

N^G,N^G-dimethylarginine dimethylaminohydrolases (DDAHs) are the enzymes responsible for hydrolyzing asymmetric N^G,N^G-dimethylarginine (ADMA), a metabolite generated by the action of type 1 protein arginine N-methyltransferases [4]. In the cells, ADMA is an endogenous inhibitor of nitric oxide synthase (NOS) which generates nitric oxide (NO) [5]. In thermogenic adipocytes, NO activates soluble guanylyl cyclase increasing the cellular level of cyclic guanosine monophosphate (cGMP) [6], which in turn, activates protein kinase G (PKG) [7]. cGMP-mediated PKG activation has been reported to stimulate a thermogenic program in adipocytes [8]. However, the role of DDAHs has not been explained yet for thermogenic adipocytes.

Activation of ADRB3 by its specific agonists was expected to be a promising strategy for anti-obesity. However, recent clinical trials using mirabegron, an ADRB3 specific agonist, turned the effectiveness out to be discouraging in human cases [3]. Furthermore, Valentine et al, described that prolonged administration of an ADRB3 agonist causes catecholamine resistance [9], suggesting alternative strategies to activate thermogenic adipocytes would be required. Given the established role of DDAHs, we hypothesized that increased expression of DDAHs could activate thermogenic adipocytes through PKG signaling, and we examined the role of DDAHs by employing adipocyte-specific DDAH1 knockout and overexpressing mice.

2. Results

This article is protected by copyright. All rights reserved.

Author Manuscript

2.1 Adipocyte-specific *Ddah1* deletion does not affect thermogenic gene expression.

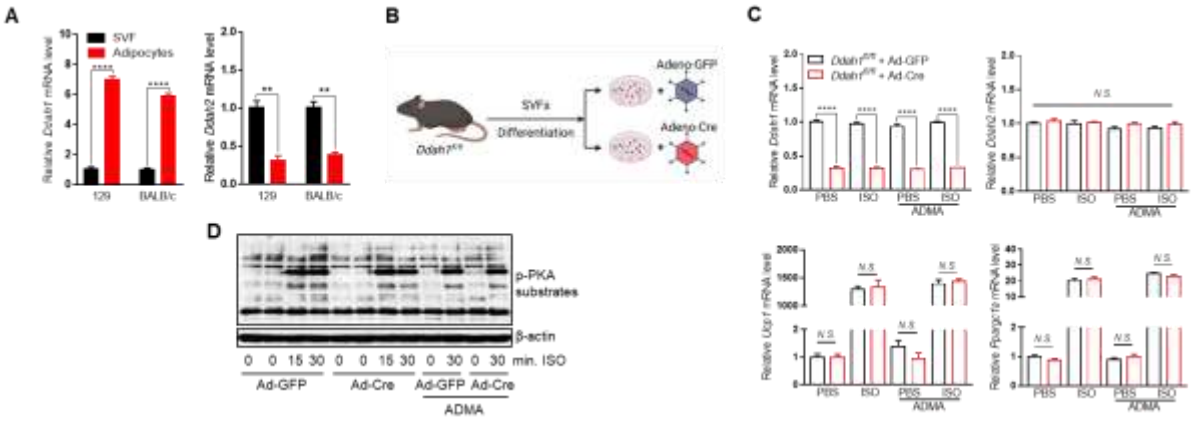


Figure 1. DDAH1 deletion does not affect thermogenic gene expression in primary iWAT cells. (A) *Ddah1* and *Ddah2* mRNA levels in SVFs and mature adipocytes of iWAT from 129 (n=3 mice) or BALB/c mice (n=3 mice). (B) Schematic description of the experiment. SVFs isolated from iWAT of *Ddah1*$^{fl/fl}$ mice were differentiated to adipocytes and infected with Adenovirus expressing GFP (Ad-GFP) or Cre-recombinase (Ad-Cre), followed by combinational treatment of ADMA (10 μM for 16 h pretreatment) and isoproterenol (ISO; 10 μM for 5 h for qPCR). (C) mRNA levels of *Ddah1*, *Ddah2*, *Ucp1* and *Ppargc1a* in the differentiated adipocytes (n=3 per group). The values are presented as means±SEM. **p*<0.05, ***p*<0.01 and *****p*<0.0001. *N.S.*=not significant. (D) Representative immunoblot of the differentiated adipocytes. ADMA (10 μM) was pretreated for 16 h prior to ISO (10 μM) treatment for indicated time intervals. β-actin was used as a loading control.

DDAHs expression in adipocytes has not been previously evaluated [10]. We therefore analyzed the mRNA levels of *Ddah1* and *Ddah2* in stromal vascular fractions (SVFs) and mature adipocytes of iWAT. In two widely used mouse strains, 129 and BALB/c, *Ddah1* mRNA expression was more abundant in mature adipocytes, whereas *Ddah2* mRNA expression was in SVFs, implying that DDAH1 is more likely to have an important role in adipocytes (Figure 1A). To evaluate the role of DDAH1 in adipocytes, we generated adipocyte-specific *Ddah1* knockout mice by crossing *Ddah1*$^{fl/fl}$ mice with adiponectin-Cre recombinase (AQ-Cre) mice, whose expression is under the control of the adiponectin promoter. Unexpectedly, *Ddah1* was not observed to be deleted in interscapular brown adipose tissue (iBAT), iWAT and eWAT under basal conditions (Figure S1A, Supporting information). In contrast, it was partially deleted in iWAT, when the mice were exposed to cold (Figure S1B, Supporting information), and the gene deletion was facilitated in iBAT and iWAT by

This article is protected by copyright. All rights reserved.

Author Manuscript

administration of an ADRB3 specific agonist, CL-316,243 (Figure S1C, Supporting information). However, *Ddah1* deletion did not affect *Ucp1* expression in all three fat depots (Figure S1B,C, Supporting information).

Because *Ddah1* knockout was unseccessful, we opted for an alternative strategy: we used the CRISPR-associated protein 9 (Cas9)-guide RNA (gRNA) system, which is applicable to adipocytes [11]. AAV-gRNA targeting *Ddah1* was administered to mice expressing Cas9 specifically in adipocytes (Figure S2A, Supporting information). However, we found that DDAH1 levels were not altered at the mRNA and protein levels, indicating that *Ddah1* was not deleted (Figure S2B,C, Supporting information). To further validate the adipocyte-specific knockout of *Ddah1*, mice were injected with CL-316,243, and subsequently, mature adipocytes were isolated. Nevertheless, the DDAH1 protein levels were not altered (Figure S2D, Supporting information).

In the *Ddah1* knockout mice obtained using the Cre-LoxP system, approximately 50% *Ddah1* deletion was achieved after stimulation. To examine it more clearly, primary iWAT cells were prepared from *Ddah1*$^{fl/fl}$ mice and infected with adenovirus expressing green fluorescent protein (Ad-GFP) or Cre recombinase (Ad-Cre; Figure 1B). *Ddah1* was knocked out approximately 70% in these primary iWAT cells after Ad-Cre infection (Figure 1C). However, *Ucp1* and *Ppargc1a* mRNA expressions were unchanged either in basal or under a stimulus condition with isoproterenol (ISO; a nonselective agonist for β-adrenergic receptors) in the *Ddah1* knockout cells (Figure 1C). Given its enzymatic role, DDAH1 is presumably only effective in the presence of ADMA [12]. However, neither thermogenic gene expression nor PKA activity, as determined by phosphorylation of PKA substrates, were affected by *Ddah1* knockout in ADMA treated cells (Figure 1C,D).

2.2 Adipocyte-specific DDAH1 overexpressing mice have comparable phenotypes to control mice

This article is protected by copyright. All rights reserved.

Author Manuscript

Although adipocyte-specific *Ddah1* knockout mice did not exhibit the expected phenotypes, stimulation of the DDAH1 signal cascade, which has the potential to increase PKG activity instead of the ADRB3-PKA axis, is still attractive for consistently activating thermogenesis. For this purpose, we generated adipocyte-specific DDAH1 overexpressing mice using an AAV-DIO system (Figure 2A) [13]. As expected, expressions of exogenous DDAH1 tagged with FLAG, were only observed in the iBAT, iWAT and eWAT, but not in other tissues, in an AQ-Cre dependent manner (Figure 2B,J). However, the body weights and histology of the adipose tissues of the adipocyte-specific DDAH1 overexpressing mice were comparable to those of the control mice, and the mRNA expression levels of thermogenic genes and electron transport chain (ETC)-related genes were not altered (Figure 2C-F). In addition, protein expressions of UCP1, OXPHOS and PKA activity remained unchanged in adipose tissues (Figure 2G). Notably, the concentration of proteins that are asymmetrically dimethylated on arginine residues were not reduced, and phospho-vasodilator-stimulated phosphoprotein (p-VASP), a substance of PKG [14], was not increased by DDAH1 overexpression (Figure 2G). Moreover, the NO levels in adipose tissues were not affected by DDAH1 overexpression (Figure 2H). These results indicate that DDAH1 delivery targeting adipocytes does

This article is protected by copyright. All rights reserved.

Author Manuscript

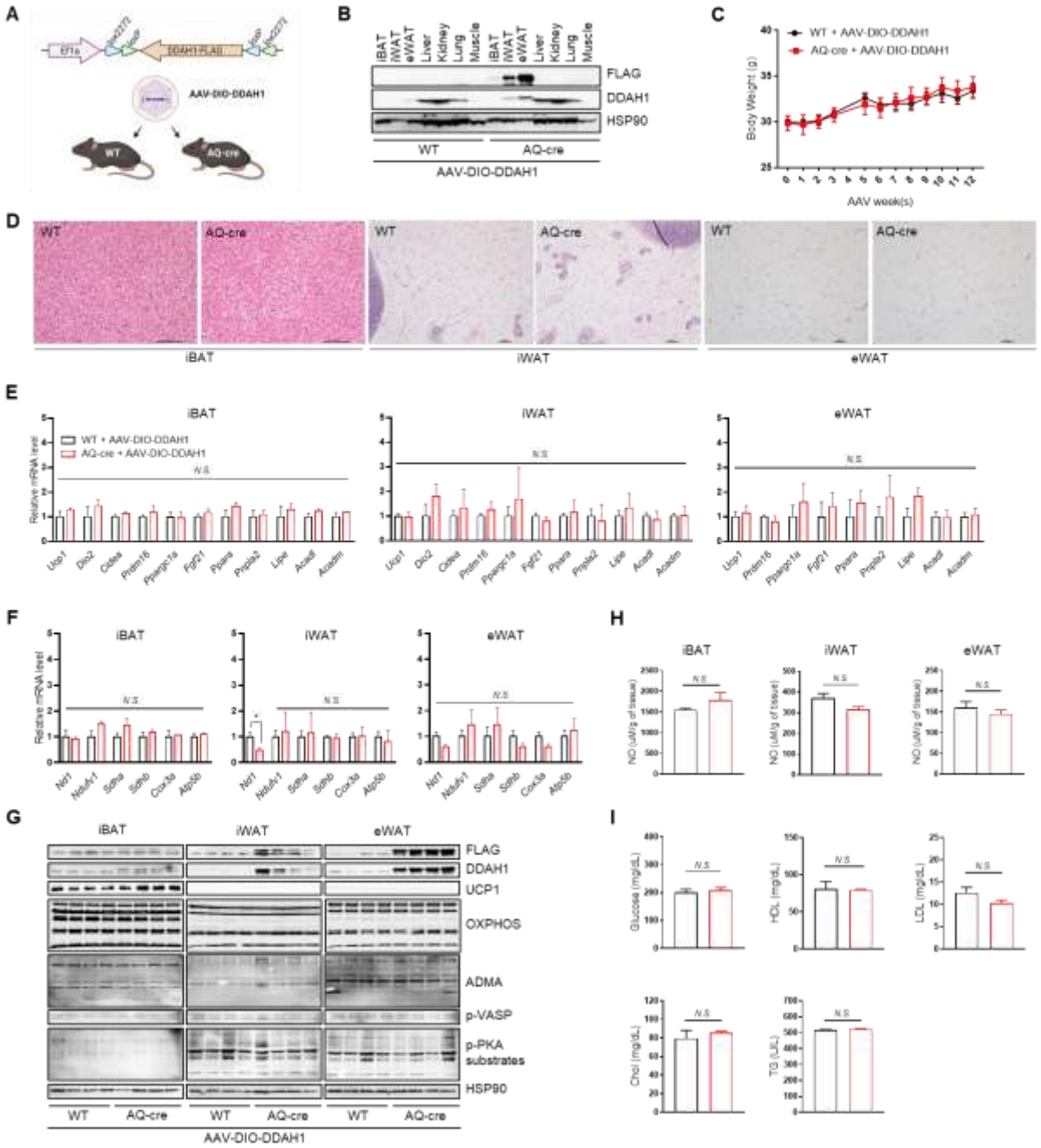


Figure 2. Adipocyte-specific DDAH1 overexpressing mice have comparable phenotypes to control mice under basal conditions. (A) Schematic description of the experiment. Wild type or AQ-cre mice were intraperitoneally administered AAV-DIO-DDAH1 and housed at room temperature. (B) Immunoblot analysis to confirm DDAH1 transduction in fat tissues at three weeks post virus injection. HSP90 was used as a loading control. (C) Body weights before and after virus injection (WT + AAV-DIO-DDAH1, n=4; AQ-cre + AAV-DIO-DDAH1, n=4). (D) Histological images of the adipose tissues (WT, n=5; AQ-cre, n=4). Representative images are presented. Scale bar=100 μm. (E,F) mRNA levels of indicated genes in iBAT, iWAT and eWAT of the mice (WT, n=4; AQ-cre, n=4). (G) Immunoblots of the indicated proteins in iBAT, iWAT and eWAT of the mice. HSP90 was used as a loading control. (H) Nitric oxide levels in iBAT, iWAT and eWAT (WT, n=3; AQ-cre, n=5). (I) Serum chemistries of the mice (WT, n=4; AQ-cre, n=4; HDL, High Density Lipoprotein; LDL, Low Density Lipoprotein; Chol, Cholesterol; TG, Triglyceride). Two-way

This article is protected by copyright. All rights reserved.

Author Manuscript

ANOVA (C) and Student's t-test (E, F, H, I) were used to conduct statistical analysis. The values are presented as means±SEM. *N.S.*=not significant.

not contribute to activation of thermogenesis or weight loss. This is further supported by the unchanged levels of glucose, HDL, LDL, cholesterol and triglyceride in sera, hepatic morphologies, and the metabolic gene expression in the liver of adipocyte-specific *Ddah1* knockout mice (Figure 2I, Figure S3, Supporting information).

2.3 Cold- and diet-induced thermogenesis is not reinforced in adipocyte-specific DDAH1 overexpressing mice

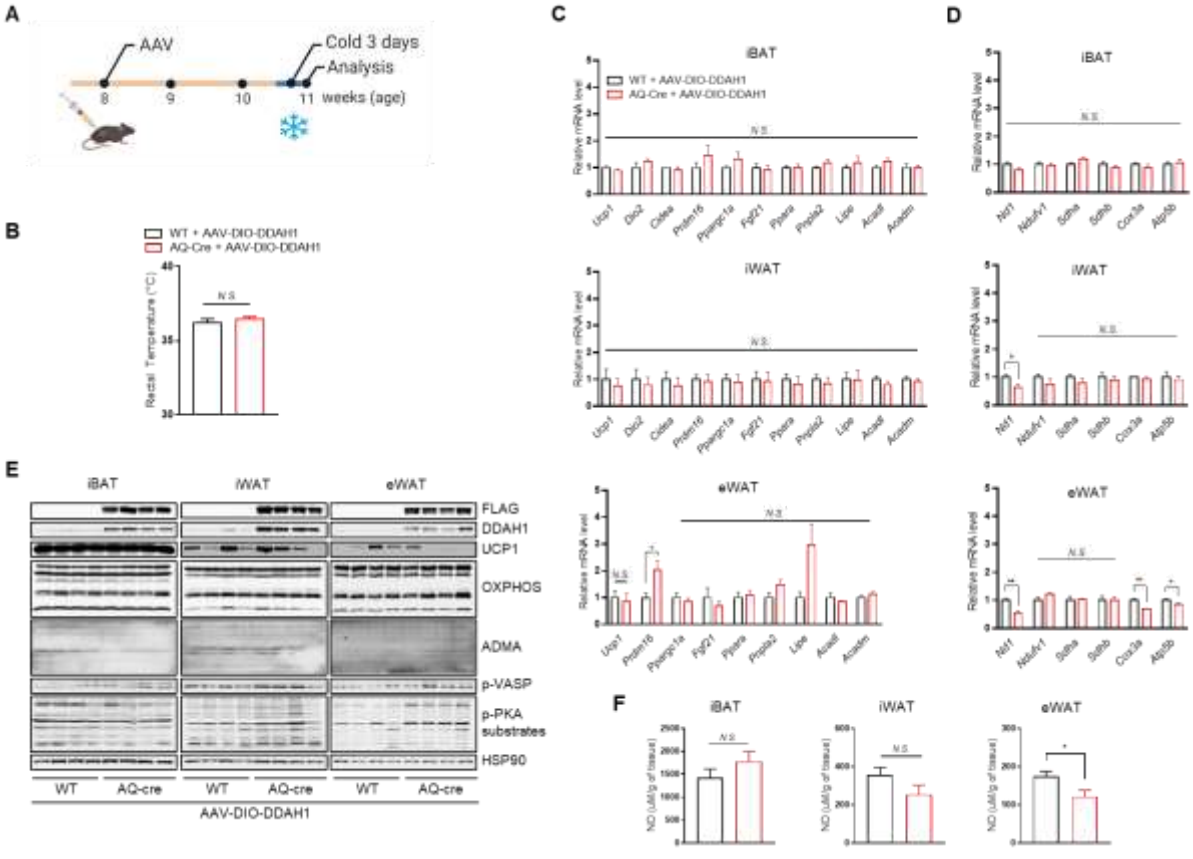


Figure 3. Cold-induced thermogenesis is not reinforced in adipocyte-specific DDAH1 overexpressing mice. (A) Schematic description of the experiment. Mice were injected intraperitoneally with AAV-DIO-DDAH1. Mice were housed at 4℃ at two weeks post virus injection

This article is protected by copyright. All rights reserved.

Author Manuscript

for three days. (B) Rectal temperature was measured using a digital thermometer (WT + AAV-DIO-DDAH1, n=4; AQ-cre + AAV-DIO-DDAH1, n=5). (C,D) mRNA levels of the indicated genes in iBAT, iWAT and eWAT of the mice exposed to cold (WT, n=4; AQ-cre, n=5). (E) Immunoblot analysis of the indicated proteins in iBAT, iWAT and eWAT of the mice. HSP90 was used as a loading control. (F) Nitric oxide levels in adipose tissues (WT, n=4; AQ-cre, n=4). The values are presented as means±SEM. *p<0.05 and **p<0.01. *N.S.*=not significant.

To further evaluate the thermogenic potential of DDAH1, adipocyte-specific DDAH1 overexpressing mice were exposed to 4°C for three days (Figure 3A). After three days of cold exposure, the rectal temperature of the DDAH1 overexpressing mice was similar to control mice, and the overall expressions of thermogenic and ETC-related genes were also unchanged (Figure 3B-D). Consistent with gene expression, amounts of thermogenic proteins, ADMA and p-VASP were not altered in the fat tissue of adipocyte-specific DDAH1 overexpressing mice (Figure 3E). Furthermore, the NO levels were unchanged in the iBAT and iWAT, and they were rather decreased in the eWAT of DDAH1 overexpressing mice (Figure 3F).

This article is protected by copyright. All rights reserved.

Author Manuscript

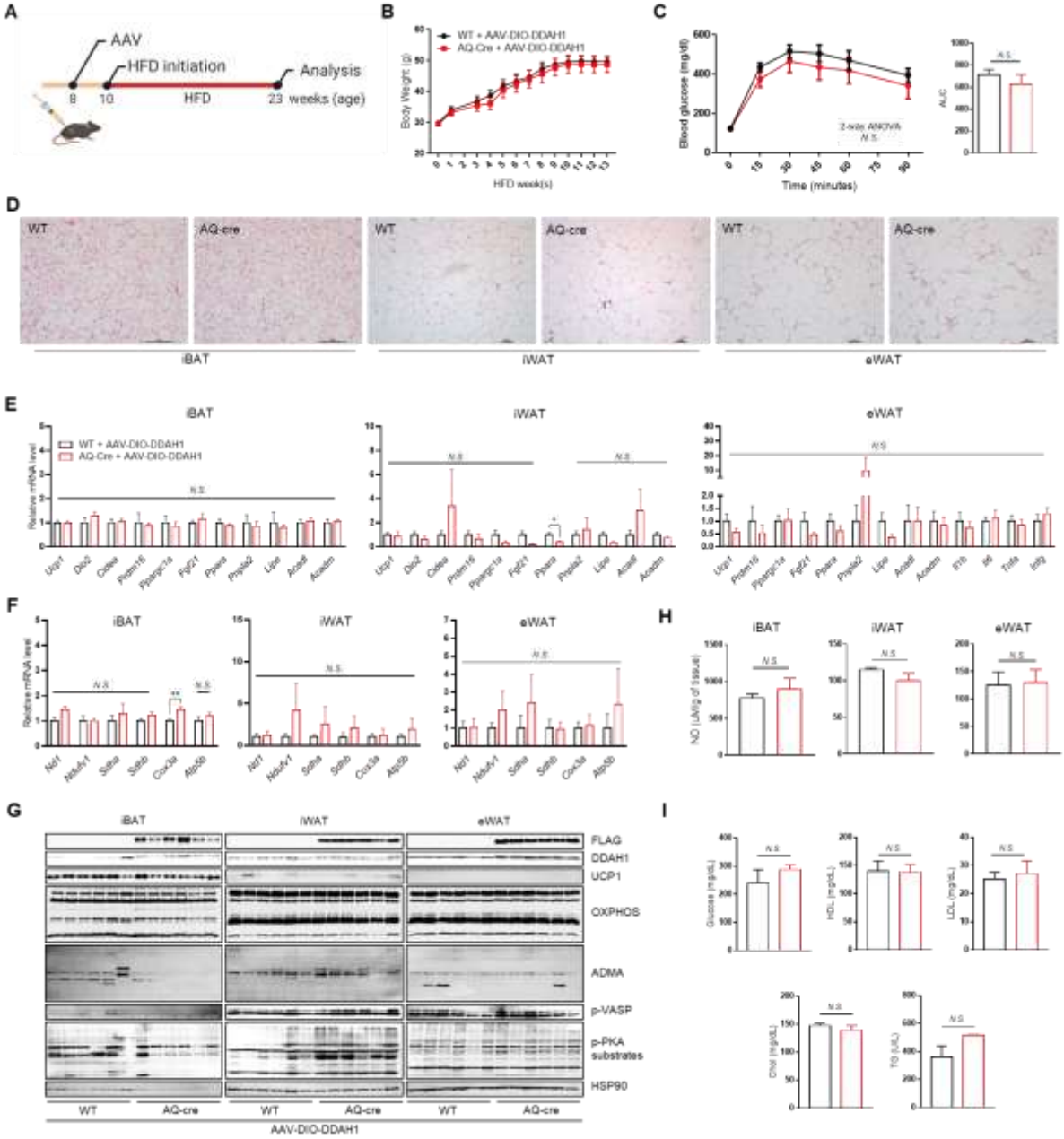


Figure 4. Diet-induced thermogenesis is not supported in adipocyte-specific DDAH1 overexpressing mice. (A) Schematic description of the experiment. Mice were intraperitoneally injected with AAV-DIO-DDAH1, followed by HFD feeding for 13 weeks from week 2 post virus injection. (B) Body weights of the mice (WT + AAV-DIO-DDAH1, n=7; AQ+AAV-DIO-DDAH1, n=6). (C) Blood glucose concentrations from the glucose tolerance test (left panel) and area under curve (right panel). (D) Histological images of the adipose tissues (WT, n=5; AQ-cre, n=4). Representative images are presented. Scale bar=100 μm. (E,F) mRNA amounts of the indicated genes in iBAT, iWAT and eWAT of the mice fed HFD (WT, n=7; AQ-cre, n=6). (G) Immunoblot analysis of the indicated proteins in iBAT, iWAT and eWAT. HSP90 was used as a loading control. (H) Nitric oxide levels in adipose tissues (WT, n=5; AQ-cre, n=4). (I) Serum chemistries of the mice (WT, n=7; AQ-cre, n=6; HDL, High Density Lipoprotein; LDL, Low Density Lipoprotein; Chol, Cholesterol; TG, Triglyceride). Two-way ANOVA (B, C) and Student's t-test (C, E, F, H, I) were used to conduct

This article is protected by copyright. All rights reserved.

Author Manuscript

statistical analysis. The values are presented as means±SEM. *p<0.05, **p<0.01, and *N.S.*=not significant.

We next evaluated if DDAH1 had a protective effect on diet-induced obesity (Figure 4A). After 11 weeks of HFD, body weights were similar between groups and glucose tolerance was not improved (Figure 4B,C). The histology of the adipose tissues and the expression levels of thermogenic and ETC-related genes were also unchanged by adipocyte-specific DDAH1 overexpression (Figure 4D-F). Concentrations of thermogenic proteins, ADMA and p-VASP, and NO levels were unaffected (Figure 4G,H). Although increased PKA activity was observed in iWAT of adipocyte-specific DDAH1 overexpressing mice (Figure 4 G), it was not sufficient to ameliorate the deteriorated indices of serum chemistries of the mice fed HFD and HFD-induced hepatic steatosis (Figure 4I, Figure S4, Supporting information).

3. Discussion

Strategies to activate thermogenic adipocytes are gaining attention for their potential to contribute to consume surplus energy both in mice and humans. One of the most convincing ways to achieve that would be activation of ADRB3, the most upstream molecule in the classical signaling cascade of thermogenesis by the sympathetic nerve system. However, clinical trials with chronic mirabegron administration revealed that its effect is not sufficient for humans to lose body weight [3a]. The possibility for ADRB3 activation to develop atherosclerotic plaques as a side effect also has to be mentioned [15]. Moreover, sustained treatment with ADRB3 agonists could lead to catecholamine resistance, characterized by ADRB3 reduction [9, 16]. Hence, development of an alternative strategy, rather than ADRB3 activation, might be necessary.

We sought an alternative factor that could stimulate the NO-cGMP-PKG axis to activate thermogenesis in brown and beige adipocytes [17]. In the present study, we focused on a feasible

This article is protected by copyright. All rights reserved.

Author Manuscript

candidate, DDAH1, given that it increases NO by breaking down ADMA and that its role in thermogenic adipocytes has not been evaluated. Although DDAH1 is relatively abundant in kidney [10], we found it is also expressed in adipocytes of iBAT, iWAT and eWAT with a preference in mature adipocytes than SVFs, leading us to generate adipocyte-specific *Ddah1* knockout mice to investigate its role. However, under basal conditions, *Ddah1* knockout was not evident in adipose tissue, likely due to the limited accessibility of Cre recombinase to the chromosomal location of the *Ddah1* gene, particularly exon 4 where the LoxP sites were inserted. Unlike this, a partial but significant deletion of the *Ddah1* gene was observed under stimulus conditions such as cold exposure or CL-316,243 administration, suggesting a conformational change of the chromosome makes Cre recombinase to be accessible [18]. Notably, the floxed *Ddah1* was clearly knocked out in primary iWAT cells infected with Ad-Cre (Figure 1C). We also attempted to knock *Ddah1* out using the Cas9-gRNA system, which targeted exon 1 of the *Ddah1 gene* (Figure S2, Supporting information). However, DDAH1 expression in adipocytes remained intact, suggesting limited access of Cas9 to this region. Targeting other exons may be required for the complete knockout of *Ddah1* to identify its pathophysiological roles.

Decreased DDAH1 expression is related to the onset and progression of diseases associated with endothelial dysfunction [19]. Vascular endothelial-specific *Ddah1* knockout mice exhibit increased ADMA, which was associated with increased systolic blood pressure in those mice [20]. However, the role of DDAH1 in thermogenic adipocytes has not been revealed. In the present study, adipocyte-specific DDAH1 overexpressing mice possessed a comparable ADMA concentration in adipose tissues (Figure 2G). Moreover, ADMA treatment did not affect the mRNA expressions of *Ucp1* and *Ppargc1a* as well as PKA activity in primary iWAT cells of the *Ddah1* knockout mice (Figure 1C, D), suggesting that the DDAH1-ADMA axis is not a critical regulator for thermogenesis. This hypothesis was further supported by the adipocyte-specific knockout mice of *protein arginine methyltransferase 1* (*Prmt1*), which is one of the enzymes responsible for ADMA generation [4b], rather leading to the impairment of thermogenic gene expressions during cold exposure [21].

This article is protected by copyright. All rights reserved.

Author Manuscript

In this study, we generated adipocyte-specific DDAH1 overexpressing mice using AAV-DIO (also called a flip-excision; FLEX) system [13]. This advanced system allows us to generate highly specific-adipocyte DDAH1 overexpressing mice, without expression in other tissues (Figure 2B, G). In addition, because exogenous DDAH1 expression was initiated via AAV injection at the adult stage, any unintended effects of DDAH1 overexpression on developmental stage could be excluded. Although the expression of exogenous DDAH1 was relatively abundant in eWAT, significant amounts of DDAH1 were present in iBAT and iWAT as well (Figure 2G). Despite the overexpression, the levels of most of thermogenic and mitochondrial genes and proteins exhibited no alterations under basal, cold exposure or HFD conditions. Moreover, the HFD-induced glucose tolerance and the values of serum chemistries were not improved in adipocyte-specific DDAH1 overexpressing mice. These results suggest that DDAH1 gene therapy targeting adipocytes may not be effective.

In summary, adipocyte-specific *Ddah1* deletion does not change *Ucp1* expression, and we were not able to find any evidence that adipocyte-specific DDAH1 overexpressing mice exhibit enhanced activation of thermogenic adipocytes during either cold exposure or HFD. Thus, we conclude that DDAH1 is dispensable for cold- or diet-induced thermogenesis.

4. Experimental Section

4.1 Animals

All animal experiments were approved by the Institutional Animal Care and Use Committee of Chonnam University (#CNU IACUC-YB-2023-21). *Ddah1* knockout mice (*Ddah1*$^{fl/fl}$ *AQ-cre*) were generated by crossing *Ddah1*$^{fl/fl}$ (#026756, Jackson Laboratory, Bar Harbor ME; LoxP sites in exon 4) with adiponectin-Cre mice (#028020, Jackson Laboratory). Basically, the mice were maintained on an *ad libitum* chow diet under a 12h light/12h dark cycle at 22°C with 55±5% relative humidity. For cold

This article is protected by copyright. All rights reserved.

Author Manuscript

exposure experiments, single-housed mice were placed at 4°C for three days. For activation of β3-adrenergic receptor, mice were injected with CL-316,243 (1 mg/kg; C5976, Sigma) intraperitoneally for four consecutive days. Rectal temperature was measured with a digital thermometer (#THS-232-107, Thermoworks) three hours prior sacrificing the mice.

For *Ddah1* knockout using the Cas9-gRNA system, Rosa26-LSL-Cas9 mice (#026175, Jackson Laboratory, Bar Harbor ME) were purchased and crossed with AQ-cre mice to generate Rosa26-LSL-Cas9 with or without AQ-cre mice. A *Ddah1* gRNA was designed using an in-silico sgRNA design tool, CRISPick68, and chosen with the least mismatched off-target sites criteria. The gRNA sequences chosen were as follows: gRNA #1 forward 5'-ACCGCCCGACTGCGTGTTCGTGG-3' and reverse 5'-AACCCACGAACACGCAGTCGGGC-3'; gRNA #2 forward 5'-ACCGCGCCAGCACGAGCTCTACGT-3' and reverse 5'-AACACGTAGAGCTCGTGCTGGCGC-3'. The gRNAs were synthesized (Bionics) and inserted into a pAAV-U6-sgRNA-CMV-mCherry vector which was generated by fusing two different vectors (#87916, #85451, Addgene).

Adipocyte-specific DDAH1 overexpressing mice were generated by administration of AAV expressing DDAH1 in a Cre recombinase dependent manner (AAV-DIO-DDAH1) using AQ-cre mice. Wild-type or AQ-cre mice were intraperitoneally injected with the AAV-DIO-DDAH1 virus (4 x 10^{12} virus particles per mouse in 500 μL volume). For diet-induced obesity, mice were fed an HFD (60% of calories from fat; #D12492, Research Diets). For the glucose tolerance test, mice undergoing an HFD for eleven weeks were fasted for 16 hours and administered glucose solution (2 g/kg body weight) intraperitoneally. A drop of blood from the tail vein was measured with Accu-Chek Performa (Roche) at each time point.

4.2 Isolation of mature adipocytes and stromal vascular fractions, and primary cell culture

This article is protected by copyright. All rights reserved.

Author Manuscript

To obtain mature adipocytes and SVFs, iWAT were isolated, minced into small pieces, and digested with collagenase D/Dispase II (#11088882001, #4942078, Roche). Cell suspensions in Dulbecco's Modified Eagle Medium/Nutrient Mixture F-12 (DMEM/F12) (#10565018, ThermoFisher Scientific) containing 10% fetal bovine serum (FBS; #F2442, Sigma-Aldrich) were filtered through a 100 μm nylon filter to remove debris. The resulting liquid was centrifuged at 1,000 rpm for 10 min at room temperature and the floating mature adipocytes were collected. Pellet was resuspended and re-filtered through a 40 μm nylon filter, followed by a second centrifugation. Pelleted SVFs were collected and further processed for mRNA extraction. For adipocyte differentiation, SVFs were seeded on collagen coated plates and stimulated with DMEM/F12 media supplemented with 10% FBS, 1 μM dexamethasone (#D4902, Sigma-Aldrich), 0.5 mM 3-isobutyl-1-methyxanthine (IBMX; #I7018, Sigma-Aldrich), 1 μg/mL insulin (#I5500, Sigma-Aldrich), 1 μM rosiglitazone (#71740, Cayman), and penicillin/streptomycin (#15140122, Life Tech) for two days. Then, the media were replaced with a differentiation medium (DMEM/F12 supplemented with 10% FBS, 1 μg/mL insulin, and penicillin/streptomycin). The media were changed every other day until before harvest. Cells were treated with ADMA (#D4268, Sigma-Aldrich) and isoproterenol hydrochloride (#I6504, Sigma-Aldrich).

4.3 AAV production

For an adipocyte-specific overexpression of DDAH1, we employed an AAV-DIO system, and AAV were prepared as described previously with minor modifications [22]. AAV-FLEX-mDDAH1-FLAG plasmid was synthesized in Vectorbuilder (IL, USA) and co-transfected with pAAV2/8 (#112864, Addgene) and helper plasmid pAdDelta6 (#112867, Addgene) into 293T cells in a 1:1:1 molar ratio using polyetherimide. Briefly, the cells containing viral particles were harvested at 60 h post-transfection and lysed in AAV lysis buffer (150 mM NaCl, 20mM Tris pH 8.0) through three cycles of freezing and thawing, followed by incubation with Benzonase (#8263, Sigma-Aldrich). The

This article is protected by copyright. All rights reserved.

Author Manuscript

supernatant containing viruses was purified using an iodixanol gradient solution and high-speed centrifuge. The viral fraction was concentrated using an Amicon Ultra-15 Centrifugal Filter Unit (#UFC910096, Sigma-Aldrich) and washed two times with PBS containing 0.1% Poloxamer 188 (#P5556, Sigma-Aldrich) and three times with PBS. Five microliters of each virus were incubated with DNase and proteinase K serially and then, the number of virus particles of an AAV was determined by quantitative PCR (#CFX96, Bio-Rad).

4.4 Serum analysis

Serum collected from euthanized mice was stored at -80°C before analysis. Serum concentrations of glucose (GLU: #1112111), high-density lipoprotein (HDL-C: #1152112), low-density lipoprotein (LDL-C: #1172112), cholesterol (CHOL: #1212106) and triglycerides (TG: #1222111) were measured using an auto chemistry analyzer (#Dotto 2000, MTD Medical System, Co.)

4.5 Immunoblot analysis

Mouse tissues were homogenized in radioimmunoprecipitation buffer (150 mM NaCl, 50 mM Tris, pH 8.0, 0.5% sodium deoxycholate, 0.1% sodium dodecyl sulfate, and 1x NP-40) containing a protease inhibitor cocktail (#11836153001, Sigma-Aldrich). Protein concentrations were quantified using DC Protein Assay Reagents (#5000116, Bio-Rad). Equal amounts of each sample protein were subjected to acetone precipitation for sample cleaning as described earlier [23], and the protein pellet after the process was resuspended in SDS sample buffer (60 mM Tris pH 6.8, 25% glycerol, 0.1% bromophenol blue, 2% SDS, 2.5% 2-mercaptoethanol). Samples were conducted via sodium dodecyl sulfate-polyacrylamide gel electrophoresis and transferred onto nitrocellulose membranes. The blots were incubated with antibodies against either β-actin (#8457, Cell Signaling Technology), ADMA (#13522, Cell Signaling Technology), DDAH1 (#PA5-52278, ThermoFisher Scientific), FLAG

This article is protected by copyright. All rights reserved.

Author Manuscript

(#PA1-984B, ThermoFisher Scientific), HSP90 (#4874, Cell Signaling Technology), OXPHOS (#ab110411, Abcam), p-PKA substrates (#9621, Cell Signaling Technology), p-VASP (#3114, Cell Signaling Technology), or UCP1 (#ab10983, Abcam). Proteins were visualized using a luminescent image analyzer (#ImageQuant LAS 4000 mini, GE Healthcare) with horseradish peroxidase-conjugated secondary antibodies (#7074, #7076, Cell Signaling Technology).

4.6 Quantification of mRNA

Total RNA was isolated from mouse tissues using Tri-solution (#TS200-001, Biosolution) according to the manufacturer's instructions. For RNA isolation from the iWAT and epididymal white adipose tissue (eWAT) of HFD mice, total RNA was isolated using Tri-solution combined with RNeasy kit (#74106, Qiagen) briefly as follows: fat tissues were homogenized in Tri-solution and centrifuged at 12,000 x g for 10 min at 4℃. The interphase layers containing RNA were mixed with chloroform and centrifuged at 12,000 x g for 10 min at 4℃. The top layered solution was transferred to a new tube, mixed with an equal volume of 70% ethanol, transferred to a RNeasy mini spin column, and the manufacturer's protocol was followed from this step. Isolated RNAs were utilized to generate cDNA using Moloney murine leukemia virus reverse transcriptase (#28025013, Thermo Fisher Scientific). Sequences of the primers used in this study are as follows (in alphabetical order); *Acadl* forward 5'-TCTTTTCCTCGGAGCATGACA-3' and reverse 5'-GACCTCTCTACTCACTTCTCCAG-3'; *Acadm* forward 5'-AGGGTTTAGTTTTGAGTTGACGG -3' and reverse 5'-CCCCGCTTTTGTCATATTCCG-3'; *Acc* forward 5'-ATGGGCGGAATGGTCTCTTTC-3' and reverse 5'-TGGGGACCTTGTCTTCATCAT-3'; *Atp5b* forward 5'-GGTTCATCCTGCCAGAGACTA-3' and reverse 5'-AATCCCTCATCGAACTGGACG -3'; *Cox3a* forward 5'-GCAGGATTCTTCTGAGCGTTCT-3' and reverse 5'-GTCAGCAGCCTCCTAGATCATGT-3'; *Dgat1* forward 5'-GGAATATCCCCGTGCACAA-3' and reverse 5'-CATTTGCTGCTGCCATGTC-3'; *Fasn* forward 5'-GGAGGTGGTGATAGCCGGTAT-

This article is protected by copyright. All rights reserved.

Author Manuscript

3' and reverse 5'-TGGGTAATCCATAGAGCCCAG-3'; *Fgf21* forward 5'-GTGTCAAAGCCTCTAGGTTTCTT-3' and reverse 5'-GGTACACATTGTAACCGTCCTC-3'; *G6pc* forward 5'-CGACTCGCTATCTCCAAGTGA-3' and reverse 5'-GTTGAACCAGTCTCCGACCA-3'; *Il1b* forward 5'-GCAACTGTTCCTGAACTCAACT-3' and reverse 5'-ATCTTTTGGGGTCCGTCAACT-3'; *Il6* forward 5'-TAGTCCTTCCTACCCCAATTTCC-3' and reverse 5'-TTGGTCCTTAGCCACTCCTTC-3'; *Infg* forward 5'-ATGAACGCTACACACTGCATC-3' and reverse 5'-CCATCCTTTTGCCAGTTCCTC-3'; *Lipe* forward 5'- GCTCATCTCCTATGACCTACGG-3' and reverse 5'-TCCGTGGATGTGAACAACCAGG-3'; *Nd1* forward 5'-GGGATAACAGCGCAATCCTA-3' and reverse 5'-ATCGTTGAACAAACGAACCA-3'; *Ndufv1* forward 5'-TTTCTCGGCGGGTTGGTTC-3' and reverse 5'-GGTTGGTAAAGATCCGGTCTTC-3'; *Pck1* forward 5'-CTGCATAACGGTCTGGACTTC-3' and reverse 5'-CAGCAACTGCCCGTACTCC-3'; *Pcx* forward 5'-CTGAAGTTCCAAACAGTTCGAGG-3' and reverse 5'-CGCACGAAACACTCGGATG-3'; *Pnpla2* forward 5'-GGATGGCGGCATTTCAGACA-3' and reverse 5'-CAAAGGGTTGGGTTGGTTCAG -3'; *Ppara* forward 5'-AGAGCCCCATCTGTCCTCTC-3' and reverse 5'-ACTGGTAGTCTGCAAAACCAAA -3'; *Ppargc1a* forward 5'-AGCCGTGACCACTGACAACGAG-3' and reverse 5'-GCTGCATGGTTCTGAGTGCTAAG-3'; *Prdm16* forward 5'- GCACGGTGAAGCCATTCATATG-3' and reverse 5'-TCGGCGTGCATCCGCTTGTG-3'; *Scd1* forward 5'-TTCTTGCGATACACTCTGGTGC-3' and reverse 5'-CGGGATTGAATGTTCTTGTCGT-3'; *Sdha* forward 5'-GGAACACTCCAAAAACAGACCT-3' and reverse 5'-CCACCACTGGGTATTGAGTAGAA-3'; *Sdhb* forward 5'-AATTTGCCATTTACCGATGGGA-3' and reverse 5'-AGCATCCAACACCATAGGTCC-3'; *Tbp* forward 5'-CCCCTTGTACCCTTCACCAAT-3' and reverse 5'-GAAGCTGCGGTACAATTCCAG-3'; *Tnfa* forward 5'-CCCTCACACTCAGATCATCTTCT-3' and reverse 5'-GCTACGACGTGGGCTACAG-

This article is protected by copyright. All rights reserved.

Author Manuscript

3'. Relative gene expression was quantified by quantitative real-time PCR (#CFX96, Bio-Rad) normalized to *TATA-box binding protein* (*Tbp*) mRNA levels.

4.7 Histological analysis

Mouse tissue samples were isolated, fixed in 10% NBF for 48 hours, dehydrated, and subsequently embedded in paraffin wax. Paraffin blocks were sectioned at thicknesses of 5 μm, mounted on slides, and stained with hematoxylin and eosin.

4.8 Nitric oxide assay

The NO levels were analyzed using the Griess reagent (#DG-NO500, DoGenBio) according to the manufacturer's instructions. Briefly, adipose tissues were homogenized in cold PBS and then, centrifuged at 10,000 x g for 5 min at 4℃. The supernatant was filtered through a 0.2 μm mesh and were subjected to the assay. After the sample reaction with Griess reagents, the absorbance was measured at 540 nm using a microplate reader, and the values were corrected based on the subjected tissue weight.

4.9 Statistical analysis

Data are expressed as mean±SEM. Asterisks indicate significant differences among the groups (*p<0.05, **p<0.01, ***p<0.001, and ****p<0.0001). Two-way analysis of variance was used to test for statistical significance among experimental groups followed by Duncan's multiple range test for multiple comparisons as a post hoc test. The data were plotted using GraphPad Prism version 9.1.1 (GraphPad Software).

Acknowledgements

This article is protected by copyright. All rights reserved.

Author Manuscript

M.-J.P. and J.L. contributed equally to this work. This research was supported by the National Research Foundation of Korea (NRF) grant funded by the Korea government (Ministry of Science and ICT, NRF-2022R1C1C1010726 and NRF-2021R1C1C2095021), the Technology Innovation Program (#20026226) funded by the Ministry of Trade, Industry & Energy (MOTIE, Korea), and Chonnam National University (Grant number: 2021-2170)

Conflict of Interest

The authors declare no conflicts of interest.

References

[1] E. T. Chouchani, L. Kazak, B. M. Spiegelman, *Cell Metab* **2019**, 29, 27.
[2] a)B. Cannon, J. Nedergaard, *Physiol Rev* **2004**, 84, 277; b)J. Wu, P. Boström, L. M. Sparks, L. Ye, J. H. Choi, A. H. Giang, M. Khandekar, K. A. Virtanen, P. Nuutila, G. Schaart, K. Huang, H. Tu, W. D. van Marken Lichtenbelt, J. Hoeks, S. Enerbäck, P. Schrauwen, B. M. Spiegelman, *Cell* **2012**, 150, 366.
[3] a)A. E. O'Mara, J. W. Johnson, J. D. Linderman, R. J. Brychta, S. McGehee, L. A. Fletcher, Y. A. Fink, D. Kapuria, T. M. Cassimatis, N. Kelsey, C. Cero, Z. A. Sater, F. Piccinini, A. S. Baskin, B. P. Leitner, H. Cai, C. M. Millo, W. Dieckmann, M. Walter, N. B. Javitt, Y. Rotman, P. J. Walter, M. Ader, R. N. Bergman, P. Herscovitch, K. Y. Chen, A. M. Cypess, *J Clin Invest* **2020**, 130, 2209; b)C. Cero, H. J. Lea, K. Y. Zhu, F. Shamsi, Y. H. Tseng, A. M. Cypess, *JCI Insight* **2021**, 6.
[4] a)T. Ogawa, M. Kimoto, K. Sasaoka, *J Biol Chem* **1989**, 264, 10205; b)M. T. Bedford, S. G. Clarke, *Mol Cell* **2009**, 33, 1.
[5] a)J. O. Lundberg, E. Weitzberg, *Cell* **2022**, 185, 2853; b)T. A. Heinrich, R. S. da Silva, K. M. Miranda, C. H. Switzer, D. A. Wink, J. M. Fukuto, *Br J Pharmacol* **2013**, 169, 1417.
[6] E. Nisoli, E. Clementi, C. Paolucci, V. Cozzi, C. Tonello, C. Sciorati, R. Bracale, A. Valerio, M. Francolini, S. Moncada, M. O. Carruba, *Science* **2003**, 299, 896.
[7] a)S. M. Kim, T. Yuen, J. Iqbal, M. R. Rubin, M. Zaidi, *Ann N Y Acad Sci* **2021**, 1487, 21; b)K. T. Ota, V. J. Pierre, J. E. Ploski, K. Queen, G. E. Schafe, *Learn Mem* **2008**, 15, 792.
[8] a)B. Haas, P. Mayer, K. Jennissen, D. Scholz, M. Berriel Diaz, W. Bloch, S. Herzig, R. Fässler, A. Pfeifer, *Sci Signal* **2009**, 2, ra78; b)D. M. Nikolic, Y. Li, S. Liu, S. Wang, *Obesity (Silver Spring)* **2011**, 19, 784.
[9] J. M. Valentine, M. Ahmadian, O. Keinan, M. Abu-Odeh, P. Zhao, X. Zhou, M. P. Keller, H. Gao, R. T. Yu, C. Liddle, M. Downes, J. Zhang, A. J. Lusis, A. D. Attie, R. M. Evans, M. Rydén, A. R. Saltiel, *J Clin Invest* **2022**, 132.
[10] J. M. Leiper, J. Santa Maria, A. Chubb, R. J. MacAllister, I. G. Charles, G. S. Whitley, P. Vallance, *Biochem J* **1999**, 343 Pt 1, 209.

This article is protected by copyright. All rights reserved.

Author Manuscript

[11] a)R. J. Platt, S. Chen, Y. Zhou, M. J. Yim, L. Swiech, H. R. Kempton, J. E. Dahlman, O. Parnas, T. M. Eisenhaure, M. Jovanovic, D. B. Graham, S. Jhunjhunwala, M. Heidenreich, R. J. Xavier, R. Langer, D. G. Anderson, N. Hacohen, A. Regev, G. Feng, P. A. Sharp, F. Zhang, *Cell* **2014**, 159, 440; b)S. M. Romanelli, K. T. Lewis, A. Nishii, A. C. Rupp, Z. Li, H. Mori, R. L. Schill, B. S. Learman, C. J. Rhodes, O. A. MacDougald, *J Biol Chem* **2021**, 297, 101402.
[12] C. T. Tran, J. M. Leiper, P. Vallance, *Atheroscler Suppl* **2003**, 4, 33.
[13] a)D. Atasoy, Y. Aponte, H. H. Su, S. M. Sternson, *J Neurosci* **2008**, 28, 7025; b)V. S. Sohal, F. Zhang, O. Yizhar, K. Deisseroth, *Nature* **2009**, 459, 698.
[14] a)E. Butt, K. Abel, M. Krieger, D. Palm, V. Hoppe, J. Hoppe, U. Walter, *J Biol Chem* **1994**, 269, 14509; b)L. Chen, G. Daum, K. Chitaley, S. A. Coats, D. F. Bowen-Pope, M. Eigenthaler, N. R. Thumati, U. Walter, A. W. Clowes, *Arterioscler Thromb Vasc Biol* **2004**, 24, 1403.
[15] W. Sui, H. Li, Y. Yang, X. Jing, F. Xue, J. Cheng, M. Dong, M. Zhang, H. Pan, Y. Chen, Y. Zhang, Q. Zhou, W. Shi, X. Wang, H. Zhang, C. Zhang, Y. Zhang, Y. Cao, *Proc Natl Acad Sci U S A* **2019**, 116, 10937.
[16] J. Mowers, M. Uhm, S. M. Reilly, J. Simon, D. Leto, S. H. Chiang, L. Chang, A. R. Saltiel, *Elife* **2013**, 2, e01119.
[17] a)M. M. Mitschke, L. S. Hoffmann, T. Gnad, D. Scholz, K. Kruithoff, P. Mayer, B. Haas, A. Sassmann, A. Pfeifer, A. Kilic, *Faseb j* **2013**, 27, 1621; b)L. D. Roberts, T. Ashmore, A. O. Kotwica, S. A. Murfitt, B. O. Fernandez, M. Feelisch, A. J. Murray, J. L. Griffin, *Diabetes* **2015**, 64, 471.
[18] M. Vooijs, J. Jonkers, A. Berns, *EMBO Rep* **2001**, 2, 292.
[19] a)K. Y. Lin, A. Ito, T. Asagami, P. S. Tsao, S. Adimoolam, M. Kimoto, H. Tsuji, G. M. Reaven, J. P. Cooke, *Circulation* **2002**, 106, 987; b)M. L. Onozato, A. Tojo, J. Leiper, T. Fujita, F. Palm, C. S. Wilcox, *Diabetes* **2008**, 57, 172; c)X. Liu, X. Xu, R. Shang, Y. Chen, *Nitric Oxide* **2018**, 78, 113.
[20] X. Hu, X. Xu, G. Zhu, D. Atzler, M. Kimoto, J. Chen, E. Schwedhelm, N. Lüneburg, R. H. Böger, P. Zhang, Y. Chen, *Circulation* **2009**, 120, 2222.
[21] X. Qiao, D. I. Kim, H. Jun, Y. Ma, A. J. Knights, M. J. Park, K. Zhu, J. H. Lipinski, J. Liao, Y. Li, S. Richard, S. A. Weinman, J. Wu, *Endocrinology* **2019**, 160, 2773.
[22] M. S. Yang, M. J. Park, J. Lee, B. Oh, K. W. Kang, Y. Kim, S. M. Lee, J. O. Lim, T. Y. Jung, J. H. Park, S. C. Park, Y. S. Lim, S. B. Hwang, K. S. Lyoo, D. I. Kim, B. Kim, *Mol Ther* **2022**, 30, 1994.
[23] M. J. Park, C. M. Lee, D. I. Kim, *Adipocyte* **2019**, 8, 357.

Activation of thermogenic adipocytes is considered as a strategy to combat obesity. Dimethylarginine dimethylaminohydrolase 1 (DDAH1) is the enzyme that potentially activates signal cascade which could turn on thermogenesis. However, roles of DDAH1 in adipocytes are not identified. This study aims to evaluate the thermogenic potential of DDAH1 using AAV-mediated adipocyte-specific gene delivery in mice.



This article is protected by copyright. All rights reserved.